

Optimal Allocation of PV Generation and Battery Storage for Enhanced Resilience

Bei Zhang, *Student Member, IEEE*, Payman Dehghanian, *Student Member, IEEE*,
and Mladen Kezunovic, *Life Fellow, IEEE*

Abstract—This paper proposes an optimal sizing and siting scheme for the battery storage and photovoltaic generation aiming at improving power system resilience. The concept of capacity accessibility for both electricity demand and non-black-start (NB-S) generating units is proposed to evaluate the reachability to the power and energy capacity during extreme events. Priority of the NB-S generating units, characterized by their different importance during the black start process, is also taken into account. The unknowable nature of the extreme events is captured and modeled through a multi-objective optimization formulation to balance three main objectives: 1) the investment and operation costs; 2) the capacity accessibility for electricity demand; and 3) the capacity accessibility for NB-S generating units. The proposed approach is validated through numerical experiments, which illustrate how the new planning approach can help enhance the grid resilience.

Index Terms—Battery storage, capacity accessibility, extreme event, photovoltaic (PV) generation, resilience.

NOMENCLATURE

Sets

K	Set of buses in the system.
L	Set of load points in the system.
NBS_G	Set of all NB-S generating units.
BS_G	Set of all B-S generating units.
ALL	Set of all generating units.
Ω	Set of different scenarios.
G	Set of all conventional generating units.

Parameters

A^s_i	Availability index of the element i during an extreme event of level s .
$A_{event,s}$	Designated system availability under an extreme event of level s .
ζ_i	Adjusting coefficient for the element i .
R^s_{i-j}	Reachability between bus i and j under $A_{event,s}$.

Manuscript received February 4, 2017; revised June 4, 2017 and August 13, 2017; accepted August 18, 2017. Date of publication August 30, 2017; date of current version December 19, 2018. This work was supported by the Qatar National Research Fund (a member of the Qatar Foundation) under Award NPRP 8-241-2-095. Paper no. TSG-00174-2017. (*Corresponding author: Bei Zhang.*)

The authors are with the Department of Electrical and Computer Engineering, Texas A&M University, College Station, TX 77843 USA (e-mail: adele.zhang@tamu.edu; payman.dehghanian@ieee.org; kezunov@ece.tamu.edu).

Color versions of one or more of the figures in this paper are available online at <http://ieeexplore.ieee.org>.

Digital Object Identifier 10.1109/TSG.2017.2747136

P^k_{Gmax}	Power capacity of the conventional generating units at bus k .
\overline{D}_l	average load at load point l .
θ_{pow}	Capacity availability factor of the battery power.
θ_{pv}	Capacity availability factor of the PV power.
θ_G	Capacity availability factor of the conventional generating unit.
$S_{k,t}$	the energy remained in the batteries on bus k at time t .
T	Total time duration.
Q_g	Prioritization factor of the NB-S generating unit g .
P_{jstart}	Cranking power needed by NB-S generating unit j .
T_{jcmx}	Critical maximum time for unit j to start up.
T_{jcmn}	Critical minimum time for unit j to start up.
Rr_i	Ramp rate of generating unit i .
T_{bl_start}	Total time of the B-S process.
T_{lctp}	Cranking time for generating unit l .
P^j_{rob}	Probability of scenario j .
r	Interest rate.
L_p	Capital longevity.
$C^{energy}_{B_in}$	Unit investment cost of the battery energy.
$C^{power}_{B_in}$	Unit investment cost of the battery power.
C_{pv_in}	Unit investment cost of the PV generation.
C_{Gi}	Marginal cost of power generation for unit i .
C_{FRUi}	Marginal cost of ramp-up service for unit i .
C_{FRDi}	Marginal cost of ramp-down service for unit i .
$C_{BG,k}$	Discharging cost of the battery storage at bus k .
$C_{BFRU,k}$	Ramp-up cost of the battery storage at bus k .
$C_{BFRD,k}$	Ramp-down cost of the battery storage at bus k .
$\xi_{B,k}$	Cost coefficient for battery degradation.
$D^j_{l,t}$	Demand at load point l at time t in scenario j .
P^{min}_{Gi}	Minimum power generation of generating unit i .
P^{max}_{Gi}	Maximum power generation of generating unit i .
Δt	Unit time interval.
$D^j_{FRU,t}$	System ramp-up and ramp-down requirement at time t in scenario j .
$D^j_{FRD,t}$	System ramp-up and ramp-down requirement at time t in scenario j .
η^-, η^+	Battery charging and discharging efficiency.
$S^j_{0,k}$	Initial state of charge (SOC) of the battery at bus k in scenario j .
S^{min}_k	Minimum battery SOC allowed at bus k .
S^{max}_k	Maximum battery SOC allowed at bus k .
\mathbf{F}^{min}	Vector of transmission line minimum capacity.
\mathbf{F}^{max}	Vector of transmission line maximum capacity.

Variables

B_{pow}^k	Power capacity of the battery storage at bus k .
B_{PV}^k	Power capacity of the PV generation at bus k .
B_{en}^k	Energy capacity of the battery storage at bus k .
t_{jstart}	Starting time of NB-S generating unit j .
t_{j1}^t	Time segment before the generating unit j starts.
t_{j3}^t	Time segment after the generating unit j reaches its maximum generation capacity.
t_{j4}^t	Time segment before the cranking power is needed for generating unit j .
w_{j1}^t	Status variable to denote the generating unit j starts to generate power.
w_{j2}^t	Status variable to denote the generating unit j reaches its maximum generation capacity.
w_{j3}^t	Status variable to denote the cranking power is needed by generating unit j .
u_{it}	Status variable to denote the unit i is started.
$P_{Gi,t}^j$	Power generation of unit i at time t in scenario j .
$FRU_{i,t}^j$	Ramp-up service of unit i at time t in scenario j .
$FRD_{i,t}^j$	Ramp-down service of unit i at time t in scenario j .
$p_{Bdis,kt}^j$	Discharging power of the battery at bus k at time t in scenario j .
$p_{Bch,kt}^j$	Charging power of the battery at bus k at time t in scenario j .
$FRU_{B,kt}^j$	Ramp-up service of the battery at bus k at time t in scenario j .
$FRD_{B,kt}^j$	Ramp-down service of the battery at bus k at time t in scenario j .
$x_{Bdis,kt}^j$	Status variables denoting whether the battery on bus k is discharging at time t in scenario j .
$x_{Bch,kt}^j$	Status variables denoting whether the battery on bus k is charging at time t in scenario j .
$P_{pv,kt}^j$	PV Power at bus k at time t in scenario j .
\mathbf{F}_t^j	Vector of the line flow at time t in scenario j .

I. INTRODUCTION

POWER grids are traditionally designed and planned to operate reliably under normal operating conditions and withstand the expected contingencies. Due to the recent years' severe events in power industry (e.g., 2011 Fukushima Daiichi nuclear disaster, 2012 Superstorm Sandy, and 2016 Hurricane Hermine with approximately 8.5 million customer power outages and direct damage amounted to \$71.4 billion in United States [1]), it has become more apparent that further considerations beyond the traditional system reliability analysis is needed for keeping the lights on at all times. New NERC power system planning performance standard TPL-0014/0040a enforced in 2016 states that "studies shall be performed to assess the impact of the extreme events [2]." The resilience is becoming an emerging topic since how the electricity grid can withstand and react to unexpected extreme events has rendered more and more criticality to people's lives and every aspect of our economy.

Recent research on power system resilience is elaborated in references [3] and [4]. In [5], the grid resilience is quantified by assessing the vulnerability of transmission lines under different loading and weather conditions. Power system resilience is a quite complicated concept with many driving factors such as generator governor actions [6], transient stability [7], physical degradation [8], etc. Resource adequacy, as another important factor influencing the grid resilience, is discussed in [9] where a deterministic approach based on the extent of the resource adequacy is adopted to examine the system resilience in face of an extreme event similar to the 2014 Polar Vortex Event [9].

As an evolving and promising resource, the PV generation and battery storage are rapidly being deployed in the grid. Compared with conventional generators, batteries are able to store the energy for use during emergencies. Besides, both the PV generation and battery storage devices can be distributed, and thus leading to a potentially higher accessibility during extreme events. Despite some disadvantages of the battery storage (e.g., limited energy capacity) and the PV generation (e.g., variable power output), their advantages still exhibit promising features during extreme events. References [10] and [11] investigate the energy not supplied (ENS) reduction through batteries. How the B-S process can be expedited by the additional battery capacity is investigated in [12]. Hence, optimal allocation of the battery storage and PV generation aiming at improving the system resilience in face of extreme events is an emerging planning problem to be solved.

Quite a few researchers have been studying the sizing and siting problem of the battery storage and the renewable resources [13]–[25], among which [13]–[16] investigate the problem in distribution systems and [17]–[24] focus on the transmission grid. The placement schemes in both distribution and transmission systems are discussed in [25]. Facilitating the grid operation is the main goal of the aforementioned research: [13] focuses on the risk-based operation of distribution companies; [14] reduces the real power loss; [15] enhances the system reliability; [18] and [19] improve the grid-scale integration of renewables; [21] alleviates the transmission congestion; and [17], [20], [22]–[25] minimize the total operation cost. Reference [16] exceptionally optimizes some mobile resources in distribution systems in preparation for a particular hurricane. The impact of such resources on enhancing the grid resilience still requires further research.

In this paper, an optimal sizing and siting scheme for the battery storage and the PV generation in the transmission network is proposed. The suggested allocation scheme extends the conventional sizing and siting paradigm [17]–[24] for accommodating battery storage and renewable resources to further improve the grid resilience in face of unknowable extreme events.

This paper is organized as follows: Section II models the *capacity accessibility*, with the concept of reachability during extreme events proposed. A new method for prioritizing the NB-S generating units is also presented in Section II. Section III proposes a multi-objective optimization model

to allocate the battery storage and PV generation aiming at improving both the *capacity accessibility* and grid operation performance. Numerical experiments are conducted and analyzed in Section IV. Section V concludes the paper and lists the contributions.

II. MODELING OF CAPACITY ACCESSIBILITY

A. Proposed Concepts

Capacity adequacy is one of the key factors playing a critical role on system resilience [9]. Higher capacity adequacy during the extreme events leads to a higher accessibility to the capacity (conventional generation, PV generation, battery energy, etc.), which renders a reduced energy not supplied (ENS), expedited B-S process, etc. during the extreme events. With rapid advancements in the control of power electronics, battery storages and PV generation are also able to provide the required reactive power [26], [27]. Coordinated with the conventional generators, their effectiveness in speeding up the system restoration is studied and proved in the past research [12], [28].

In this paper, a new metric of *capacity accessibility* during extreme events is proposed to describe the capacity adequacy status during extreme events. The *capacity accessibility* determines the extent of power and energy the grid would be able to utilize during the extreme events. The difficulty in assessing the *capacity accessibility* lies in the unknowable nature of the extreme events [29], i.e., those with low occurrence probability but high impact [3], [4]. It is almost impossible and not realistic to enumerate all the possible cases and scenarios of different extreme events. Besides, referring the extreme event to several particular kinds of contingencies may cause an inappropriate disregard of others. Differentiated from the conventional “N-m” contingency principle, we propose to emulate the extreme event based on its common impact, which is the sharp decrease in the availability of system elements, instead of specifically defining the contingency set. Extreme events under various severity levels are considered to take into account their unknowable nature.

Generally, the *capacity accessibility* depends on: (1) the size of available capacity, and (2) the *reachability* to the capacity during extreme events.

B. Reachability During Extreme Events

We quantify the *reachability* based on the common impact of the extreme events, i.e., the sharp decrease in the availability of system elements. An availability index is first assigned to each element during an extreme event, as in (1).

$$A_i^s = A_{event,s} \times \zeta_i \quad (1)$$

$A_{event,s}$ reflects the general availability of all system elements under an extreme event of level s , i.e., the more severe the extreme event is, the less likely that the device would “survive” the extreme event. In this way, extreme events can be naturally grouped into different levels characterized by different $A_{event,s}$. The lower $A_{event,s}$, the higher destructive impact the event could result in. Meanwhile, the availability of an element in face of the extreme event, A_i^s , is also affected by

its own characteristic, denoted by ζ_i , which is statistically correlated to the factors such as the equipment reliability status, its length or size/capacity, its vulnerability in some extreme conditions, etc. In other words, the availability of different elements in face of the extreme events of the same level is differentiated by ζ_i .

The *reachability* R_{i-j}^s between node i and j under $A_{event,s}$ is defined as the probability that node i and j are within the same island and, therefore, reachable to each other. In a complex system, this probability can be obtained through Monte Carlo simulations. The probability is calculated as the number of scenarios where bus i and bus j are reachable to each other, divided by the total number of simulated scenarios. The *reachability* between each set of two nodes should be calculated to evaluate the system *reachability* under an extreme event of level s , as denoted in (2), where M is the total number of nodes. Note that different values of $A_{event,s}$ can be assumed to simulate the extreme events of different levels

$$\begin{bmatrix} 1 & 2 & \cdots & i & \cdots & j & \cdots & M \\ R_{1-1}^s & R_{1-2}^s & \cdots & R_{1-i}^s & \cdots & R_{1-j}^s & \cdots & R_{1-M}^s \\ & R_{2-2}^s & \cdots & R_{2-i}^s & \cdots & R_{2-j}^s & \cdots & R_{2-M}^s \\ & & \ddots & & & & & \vdots \\ & & & R_{i-i}^s & \cdots & R_{i-j}^s & \cdots & R_{i-M}^s \\ & & & & \ddots & & & \vdots \\ & & & & & R_{j-j}^s & \cdots & R_{j-M}^s \\ & & & & & & \ddots & \vdots \\ & & & & & & & R_{M-M}^s \end{bmatrix} \begin{matrix} 1 \\ 2 \\ \vdots \\ i \\ \vdots \\ j \\ \vdots \\ M \end{matrix} \quad (2)$$

C. Capacity Accessibility for Electricity Demand

The *capacity accessibility* for electricity demand reflects the extent of capacity that can be accessible to support the load demand during the extreme event. Two types of capacity are considered: (a) power capacity and (b) energy capacity, the latter of which is specifically designed to quantify the energy stored in the battery storage, and implies how long the battery storage power can last.

Besides, there are different types of electricity demand in different load points (e.g., industrial, commercial, residential, hospitals, etc.) with various loss of load consequences. The magnitude of the load is used in this paper as the priority index, while it can be modified adaptively to account for other practical considerations. The system-wide power and energy *capacity accessibility* indices for electricity demand under an extreme event of level s are defined in (3) and (4), denoted as PCA_load^s and ECA_load^s , respectively.

$$\begin{aligned} PCA_load^s &= \frac{\sum_{k \in K} (\theta_{pow} B_{pow}^k + \theta_{pv} B_{pv}^k + \theta_G P_{Gmax}^k) \sum_{l \in L} (R_{l-k}^s \times \bar{D}_l)}{\sum_{l \in L} \bar{D}_l} \end{aligned} \quad (3)$$

$$\begin{aligned} ECA_load^s &= \left[\sum_{t=0}^{t_n} \sum_{k \in K} S_{k,t} \sum_{l \in L} (R_{l-k}^s \times \bar{D}_l) \right] / \left(T \times \sum_{l \in L} \bar{D}_l \right) \end{aligned} \quad (4)$$

In (3), the *capacity availability* factors θ_{pow} , θ_{pv} and θ_G are introduced to consider the uncertainty associated with the availability of the battery power, PV power and the power from the conventional generators, respectively. Due to the dependence on the solar irradiance, PV generation may not be able to always generate at its rated maximum capability. Such *capacity availability* factor can be calculated as the ratio of the potential maximum generation, which is constrained by the weather conditions (PV generation), available energy (battery storage) and equipment reliability (conventional generator), to the rated maximum generation within a period of time.

The *demand reachability* of bus k , under an extreme event of level s , representing the total *reachability* of the unit capacity on bus k to the entire distributed load, is defined in (5). Therefore, the PCA_load^s and ECA_load^s can be re-expressed in (6) and (7), respectively.

$$Reach_{load}^{k,s} = \left[\sum_{l \in L} (R_{l-k}^s \times \bar{D}_l) \right] / \sum_{l \in L} \bar{D}_l \quad (5)$$

$$PCA_load^s = \sum_{k \in K} (\theta_{pow} B_{pow}^k + \theta_{pv} B_{pv}^k + \theta_G P_{Gmax}^k) \times Reach_{load}^{k,s} \quad (6)$$

$$ECA_load^s = \left(\sum_{t=0}^{t_n} \sum_{k \in K} S_{k,t} \times Reach_{load}^{k,s} \right) / T. \quad (7)$$

D. Capacity Accessibility for NB-S Generating Units

Other than reducing the ENS at load points, expediting the system B-S process can also help improving the system resilience. Conventional generating units can be categorized into B-S and NB-S units. For those NB-S units, cranking power is needed to initiate the first start, while a B-S unit (e.g., hydro unit, combustion turbine) can start on its own. At the very beginning of the B-S process, the cranking power can be supplied from the B-S units, the energy stored in the battery storage, and possibly the power from the installed PV generation. Previous research demonstrated that increasing the system capability to provide the required cranking power can rapidly speed up the B-S process [12].

The system-wide *capacity accessibility* for NB-S units during an extreme event of level s is defined in (8) and (9).

$$PCA_Gen^s = \left[\sum_{k \in K} (\theta_{pow} B_{pow}^k + \theta_{pv} B_{pv}^k) \sum_{g \in NBSG} (R_{g-k}^s \times Q_g) \right] / \sum_{g \in NBSG} Q_g + \left[\sum_{h \in BSG} \theta_G P_{Gmax}^h \sum_{g \in NBSG} (R_{g-h}^s \times Q_g) \right] / \sum_{g \in NBSG} Q_g \quad (8)$$

$$ECA_Gen^s = \left[\sum_{t=0}^{t_n} \sum_{k \in K} S_{k,t} \sum_{g \in NBSG} (R_{g-k}^s \times Q_g) \right] / \left(T \times \sum_{g \in NBSG} Q_g \right) \quad (9)$$

Similarly, the generating unit *reachability* of bus k , under an extreme event of level s , is defined in (10) to reflect the *reachability* of the unit capacity at bus k to all the NB-S units.

$$Reach_{gen}^{k,s} = \left[\sum_{g \in NBSG} (R_{g-k}^s \times Q_g) \right] / \sum_{g \in NBSG} Q_g \quad (10)$$

In this paper, the priority of an NB-S unit is coupled to its importance in the B-S process, i.e., how much less the pick-up energy would be, if a given NB-S unit does not participate in the B-S process, and is defined in (11).

$$Q_g = E_{bl-start}^0 - E_{bl-start}^g \quad (11)$$

where $E_{bl-start}^0$ is the pick-up energy in the B-S process with the participation of all generating units; $E_{bl-start}^g$ is the pick-up energy with no participation of generating unit g . The evaluation of $E_{bl-start}^0$ and $E_{bl-start}^g$ depends on the sequence of the units to be turned on during the B-S process, which is reflected via variable t_{jstart} . The model presented in [30] is utilized, with some modifications, to further improve the calculation performance. The order of the unit start-up is evaluated through (12)-(13):

$$obj. \min \sum_{j \in NBSG, j \neq g} (P_{jmax} - P_{jstart}) \times t_{jstart} \quad (12)$$

$$s.t. \quad t_{jstart} \leq T_{jcmax}, \quad j \in NBSG, \quad j \neq g \quad (13.a)$$

$$t_{jstart} \geq T_{jcmin}, \quad j \in NBSG, \quad j \neq g \quad (13.b)$$

$$\sum_{\substack{i \in ALL \\ i \neq g}} Rr_i (t - t_{i1}^t - t_{i3}^t) - \sum_{j \in NBSG, j \neq g} w_{j3}^t P_{jstart} \geq 0, \\ t = 1, 2, \dots, T_{bl_start} \quad (13.c)$$

$$w_{l1}^t T_{lctp} \leq t_{l1}^t \leq T_{lctp}, \quad t = 1, 2, \dots, T_{bl_start}, \quad l \in BSG \quad (13.d)$$

$$(T_{bl_start} + 1 + T_{jctp}) w_{j1}^t - \sum_{t=1}^{T_{bl_start}} u_{jt} \leq t_{j1}^t \leq t_{jstart} + T_{jctp}, \\ t = 1, 2, \dots, T_{bl_start}, \quad j \in NBSG, \quad j \neq g \quad (13.e)$$

$$t_{j1}^t \geq 0, \quad t = 1, 2, \dots, T_{bl_start}, \quad j \in NBSG, \quad j \neq g \quad (13.f)$$

$$w_{i2}^t \cdot P_{Gi}^{max} / Rr_i \leq t - t_{i1}^t - t_{i3}^t \leq w_{i1}^t \cdot P_{Gi}^{max} / Rr_i, \\ t = 1, 2, \dots, T_{bl_start}, \quad i \in ALL, \quad i \neq g \quad (13.g)$$

$$t_{i3}^t \leq w_{i2}^t (T - T_{lctp} - P_{Gl}^{max} / Rr_l), \\ t = 1, 2, \dots, T_{bl_start}, \quad l \in BSG \quad (13.h)$$

$$t_{j3}^t \leq \sum_{t=1}^{T_{bl_start}} u_{jt} - (T_{jctp} + P_{Gj}^{max} / Rr_j + 1) w_{j2}^t, \\ t = 1, 2, \dots, T_{bl_start}, \quad j \in NBSG, \quad j \neq g \quad (13.i)$$

$$t_{j3}^t \leq w_{j2}^t T_{bl_start}, \quad t = 1, 2, \dots, T_{bl_start}, \quad j \in NBSG, \quad j \neq g \quad (13.j)$$

$$w_{j3}^t T_{bl_start} - \sum_{t=1}^{T_{bl_start}} u_{jt} \leq t_{j4}^t \leq t_{jstart} - 1, \\ t = 1, 2, \dots, T_{bl_start} \quad j \in NBSG, \quad j \neq g \quad (13.k)$$

$$t_{j4}^t \geq 0, \quad t = 1, 2, \dots, T_{bl_start}, \quad j \in NBSG, \quad j \neq g \quad (13.l)$$

$$w_{j3}^t \leq t - t_{j4}^t \leq \sum_{t=1}^{T_{bl_start}} u_{jt}, \quad t = 1, 2, \dots, T_{bl_start}, \\ j \in NBSG, \quad j \neq g \quad (13.m)$$

$$t - t_{j4}^t \leq w_{j3}^t T_{bl_start}, \quad t = 1, 2, \dots, T_{bl_start}, \\ j \in NBSG, \quad j \neq g \quad (13.n)$$

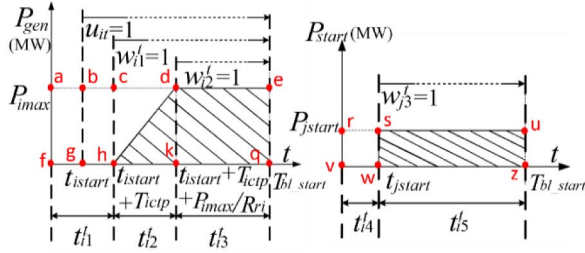


Fig. 1. Illustration of some defined variables in formulation set (13) [30].

$$w'_{jh} \leq w'_{jh}{}^{t+1}, h = 1, 2, 3, t = 1, 2, \dots, T_{bl_start} - 1, \quad j \in NBS_G, j \neq g \quad (13.o)$$

$$w'_{i2} \leq w'_{i1}, t = 1, 2, \dots, T_{bl_start}, i \in ALL, i \neq g \quad (13.p)$$

$$t'_{j1} \leq t'_{j1}{}^{t+1}, t = 1, 2, \dots, T_{bl_start} - 1, \quad j \in NBS_G, j \neq g \quad (13.q)$$

$$t'_{j3} \leq t'_{j3}{}^{t+1}, t = 1, 2, \dots, T_{bl_start} - 1, \quad j \in NBS_G, j \neq g \quad (13.r)$$

The objective (12) aims at maximizing the total generation capacity during the B-S process. Note that the generation capacity of the B-S unit within T_{bl_start} is constant, while the generation capacity of the NB-S unit can be expressed as the difference of the shaded area in the left and right charts in Fig. 1, which is $S_{deqh} - S_{suzw} = S_{dkh} + S_{deqk} - S_{suzw} = S_{dkh} + S_{aeqf} - S_{bdkg} - S_{abgf} - (S_{ruzv} - S_{rsww})$. Since some of these areas are constant and independent of t'_{jstart} , maximizing the area of $S_{deqh} - S_{suzw}$ can be transformed to minimizing the area of $S_{abgf} - S_{rsww}$, which leads to (12). Meanwhile, t'_{jstart} is assumed to be zero for all B-S units. The detailed definition of t'_{j1} , t'_{j3} , t'_{j4} , w'_{j1} , w'_{j2} , w'_{j3} , u_{it} is shown in Fig. 1 [30], where the generator output P_{gen} and the cranking power P_{start} during the start-up process are depicted.

Equations (13.a) and (13.b) limit the unit starting within the max and min critical time. The power requirement during the B-S process is described in (13.c), enforcing the generated power be greater than the cranking power needed. Equations (13.d)–(13.f) set the boundaries on the time t'_{i1} , and correlate it with w'_{i1} , which indicates that w'_{i1} becomes 1 after T_{lctp} (for B-S units) or $t'_{jstart} + T_{lctp}$ (for NB-S units). The limits on the duration $t'_{i2} = t - t'_{i1} - t'_{i3}$ and its correlation with w'_{i1} and w'_{i2} are presented in (13.g), which denotes that t'_{i2} should be 0 before w'_{i1} becomes 1 and reaches it maximum after w'_{i2} gets to 1. Equations (13.h)–(13.j) set the limits on t'_{i3} and its correlation with w'_{i2} , indicating that w'_{i2} becomes 1 and t'_{i3} starts to be non-zero after the unit reaches its maximum generation capacity. Equations (13.k) and (13.l) limit t'_{j4} with w'_{j3} for NB-S units, reflecting that t'_{j4} reaches its maximum after w'_{j3} turns to 1. The correlation of $t'_{j5} = t - t'_{j4}$ with w'_{j3} is described in (13.m) and (13.n), indicating that t'_{j5} will be non-zero after w'_{j3} turns to 1, and should be within T_{bl_start} . And (13.o)–(13.r) list the constraints on the status variables corresponding to the physical operation status. The energy that is picked up during the B-S process with no participation of unit g can be

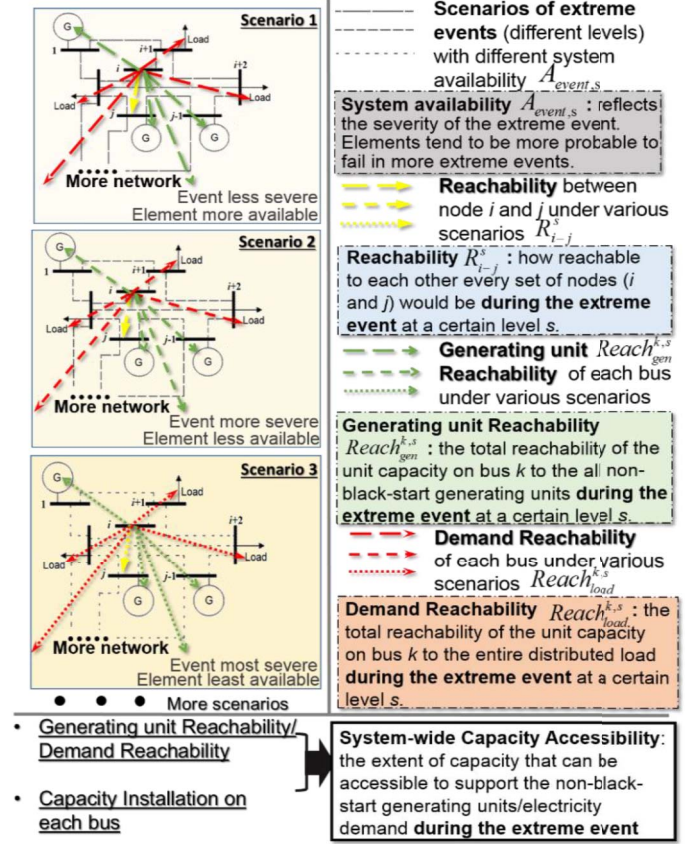


Fig. 2. Illustration of system availability, reachability, capacity accessibility.

eventually calculated in (14).

$$E_{bl_start}^g = \left\{ \begin{aligned} & \sum_{i \in ALL, i \neq g} \left[\frac{(P_{Gi}^{\max})^2}{2Rr_i} + P_{Gi}^{\max} (T_{bl_start} - T_{lctp} - P_{Gi}^{\max} / Rr_i) \right] \\ & - \sum_{\substack{j \in NBS_G, \\ j \neq g}} P_{jstart} T_{bl_start} - \left(\sum_{i \in ALL, i \neq g} P_{Gi}^{\max} t'_{istart} \right. \\ & \quad \left. - \sum_{j \in NBS_G, j \neq g} P_{Gj}^{\max} t'_{jstart} \right) \end{aligned} \right\} \quad (14)$$

Fig. 2 illustratively summarizes the concepts proposed so far: system availability, (generating unit/demand) reachability (node-based, illustratively for node i), and the capacity accessibility (system-wide). Three illustrative scenarios in terms of the extreme events of different severity levels (reflected by different system availability indices $A_{event,s}$) are presented. In a more severe extreme event (scenarios 2 and 3), the availability of the elements tends to be lower and the reachability indices also decline. However, the reachability and accessibility indices are higher (reflected by longer-dotted lines) in a less severe extreme event (scenario 1).

III. OPTIMIZATION SCHEME FOR SIZING AND SITING OF BATTERY STORAGE AND PV GENERATION

The capacity accessibility for both the electricity demand and the NB-S units (Sections III-B and III-C) can help

evaluating the capacity adequacy during an extreme event, which is one of the many factors that contribute to the system resilience. Therefore, enhancing the *capacity accessibility* when planning a system-wide allocation of battery storage and PV generation is critical for improving the system resilience.

A. Objective Functions

In order to optimally allocate the PV generation and battery storages, multi-objective optimization is adopted to simultaneously consider: (a) the investment and operation costs; (b) the *capacity accessibility* for the electricity demand; (c) the *capacity accessibility* for the NB-S units; and (d) other factors. The planning problem is to determine the power and energy capacity of the battery storage as well as the power capacity of the PV generation at each bus, denoted by B_{pow} , B_{en} , and B_{pv} , respectively. We assume that both the conventional units and the battery storages are bidding into the ramp market, which is newly proposed to accommodate the increasing net load variations and uncertainties [31].

The first objective (15.a), includes the investment cost of the battery storage and the PV generation, as well as the operation cost of the entire system, where f_{cr} is the capital recovery factor, calculated in (15.b), which converts the total investment into a stream of annual payments; t_0 and t_n are the starting and ending time of the simulations; The marginal cost of PV generation is assumed to be 0. Stochastic programming is adopted in (15) to handle the uncertainties of PV generation intermittency, where various scenarios regarding to different PV generation patterns and load profiles are considered.

$$\text{obj1. Min } \sum_{k \in K} \left[f_{cr} C_{B_in}^{energy} B_{en}^k + f_{cr} C_{B_in}^{power} B_{pow}^k + f_{cr} C_{pv_in} B_{pv}^k \right] + \sum_{j \in \Omega} P_{rob}^j \sum_{t=t_0}^{t_n} \left\{ \sum_{i \in G} \left(C_{Gi} p_{Gi,t}^j + C_{FRU_i} FRU_{i,t}^j + C_{FRD_i} FRD_{i,t}^j \right) + \sum_{k \in K} \left[C_{BG,k} p_{Bdis,kt}^j + C_{BFRU,k} FRU_{B,kt}^j + C_{BFRD,k} FRD_{B,kt}^j + \xi_{B,k} (p_{Bdis,kt}^j + p_{Bch,kt}^j) \right] \right\} \quad (15.a)$$

$$f_{cr} = r(1+r)^{L_p} / [(1+r)^{L_p} - 1] \quad (15.b)$$

The second objective is related to the contribution of the battery storage and the PV generation on the system-wide *capacity accessibility* for the demand, as described in (16).

$$\text{obj2. max PCA_load}^s \times T_{lasting} + \sum_{j \in \Omega} P_{rob}^j \times \text{ECA_load}^{s,j} \quad (16)$$

The power capacity of the conventional units is neglected from (16) as the focus is solely on the battery storage and the PV generation. Moreover, in order to combine the PCA_load and ECA_load together, a coefficient approximately denoting how long the battery power and the PV generation can last ($T_{lasting}$), is added to convert the power into energy.

Following the same principle, the third objective (17), models the contribution of the battery storage and PV on the

system-wide *capacity accessibility* for the NB-S units.

$$\text{obj3. max PCA_Gen}^s \times T_{lasting} + \sum_{j \in \Omega} P_{rob}^j \times \text{ECA_Gen}^{s,j} \quad (17)$$

The fourth objective (18) targets at improving the system reliability and represents the extensibility of modeling and incorporating additional factors in such a planning study. The expected energy not supplied (EENS), as an example, is selected here to reflect the system reliability performance.

$$\text{obj4. min EENS} = \sum_{z \in \Lambda} \sum_{k \in K} (IL_k^z \cdot \tau^z \cdot P_{rob}^z) \quad (18)$$

where IL_k^z is the interrupted load at bus k in contingency z ; P_{rob}^z denotes the occurrence probability of the contingency z ; Λ is the set of all contingencies. The model is generic and this objective can be also adjusted to consider other factors such as risk, congestion management, etc. [32], [33].

B. Constraints

The constraints of the proposed problem are as follows:

$$0 \leq p_{Bdis,kt}^j \leq x_{Bdis,kt}^j B_{pow}^k, \quad j \in \Omega, k \in K, t = t_0, t_1, \dots, t_n \quad (19.a)$$

$$0 \leq p_{Bch,kt}^j \leq x_{Bch,kt}^j B_{pow}^k, \quad j \in \Omega, k \in K, t = t_0, t_1, \dots, t_n \quad (19.b)$$

$$x_{Bdis,kt}^j + x_{Bch,kt}^j \leq 1, \quad j \in \Omega, k \in K, t = t_0, t_1, \dots, t_n \quad (19.c)$$

$$x_{Bdis,kt}^j, x_{Bch,kt}^j = 0 \text{ or } 1, \quad j \in \Omega, k \in K, t = t_0, t_1, \dots, t_n \quad (19.d)$$

$$0 \leq p_{pv,kt}^j \leq B_{pv}^k \alpha_{pv,kt}^j, \quad j \in \Omega, k \in K, t = t_0, t_1, \dots, t_n \quad (19.e)$$

$$\sum_{i \in G} p_{Gi,t}^j + \sum_{k \in K} (p_{Bdis,kt}^j + p_{pv,kt}^j) = \sum_{k \in K} p_{Bch,kt}^j + \sum_{l \in L} D_{l,t}^j, \quad j \in \Omega, t = t_0, t_1, \dots, t_n \quad (19.f)$$

$$B_{pow}^k \leq B_{en}^k \beta, k \in K \quad (19.g)$$

$$p_{Gi}^{\min} \leq p_{Gi,t}^j \leq p_{Gi}^{\max}, \quad j \in \Omega, k \in K, t = t_0, t_1, \dots, t_n \quad (19.h)$$

$$0 \leq FRU_{i,t}^j \leq Rr_i \cdot \Delta t, \quad j \in \Omega, k \in K, t = t_0, t_1, \dots, t_n \quad (19.i)$$

$$0 \leq FRD_{i,t}^j \leq Rr_i \cdot \Delta t, \quad j \in \Omega, k \in K, t = t_0, t_1, \dots, t_n \quad (19.j)$$

$$p_{Gi,t}^j + FRU_{i,t}^j \leq p_{Gi}^{\max}, \quad j \in \Omega, k \in K, t = t_0, t_1, \dots, t_n \quad (19.k)$$

$$p_{Gi,t}^j - FRD_{i,t}^j \geq p_{Gi}^{\min}, \quad j \in \Omega, k \in K, t = t_0, t_1, \dots, t_n \quad (19.l)$$

$$p_{Gi,t}^j - p_{Gi,t-1}^j \leq Rr_i \cdot \Delta t, \quad j \in \Omega, k \in K, t = t_0, t_1, \dots, t_n \quad (19.m)$$

$$p_{Gi,t-1}^j - p_{Gi,t}^j \leq Rr_i \cdot \Delta t, \quad j \in \Omega, k \in K, t = t_0, t_1, \dots, t_n \quad (19.n)$$

$$\sum_{i \in G} FRU_{i,t}^j + \sum_{k \in K} FRU_{B,kt}^j \geq D_{FRU,t}^j, \quad j \in \Omega, t = t_0, t_1, \dots, t_n \quad (19.o)$$

$$\sum_{i \in G} FRD_{i,t}^j + \sum_{k \in K} FRD_{B,kt}^j \geq D_{FRD,t}^j, \quad j \in \Omega, t = t_0, t_1, \dots, t_n \quad (19.p)$$

$$S_{k,t-1}^j - S_{k,t}^j = \left(p_{Bdis,kt}^j / \eta^+ - \eta^- p_{Bch,kt}^j \right) \cdot \Delta t, \quad j \in \Omega, k \in K, t = t_0, t_1, \dots, t_n \quad (19.q)$$

$$S_{k,t}^j \geq S_{0,k}^j B_{en}^k, \quad j \in \Omega, k \in K \quad (19.r)$$

$$S_k^{\min} B_{en}^k \leq S_{k,t}^j \leq S_k^{\max} B_{en}^k, \quad j \in \Omega, k \in K, t = t_0, t_1, \dots, t_n \quad (19.s)$$

$$p_{Bdis,kt}^j - p_{Bch,kt}^j + FRU_{B,kt}^j \leq B_{pow}^k, \quad j \in \Omega, k \in K, t = t_0, t_1, \dots, t_n \quad (19.t)$$

$$p_{Bdis,kt}^j - p_{Bch,kt}^j - FRD_{B,kt}^j \geq -B_{pow}^k, \quad j \in \Omega, k \in K, t = t_0, t_1, \dots, t_n \quad (19.u)$$

$$0 \leq FRU_{B,kt}^j \leq B_{pow}^k, j \in \Omega, k \in K, t = t_0, t_1, \dots, t_n \quad (19.v)$$

$$0 \leq FRD_{B,kt}^j \leq B_{pow}^k, j \in \Omega, k \in K, t = t_0, t_1, \dots, t_n \quad (19.w)$$

$$\mathbf{F}_{\min} \leq \mathbf{F}_t^j = \mathbf{H}\mathbf{P} \leq \mathbf{F}_{\max}, j \in \Omega, t = t_0, t_1, \dots, t_n \quad (19.x)$$

where $\alpha_{pv,kt}^j$ is the PV prediction coefficient (the percentage of the maximum output) on bus k at time t in scenario j . Further details on physical modeling of the PVs can be found in [34].

Equations (19.a)–(19.d) set the limits reflecting the fact that the battery cannot charge and discharge simultaneously. The power balance considering the possible curtailment of PV generation is modeled in (19.e) and (19.f). Coefficient β in (19.g) is to ensure that the battery generation can last for a period of time. Equations (19.h)–(19.n) set the operation conditions for the conventional units: (19.h) regulates the unit generation within its upper and lower limits; (19.i) and (19.j) set limits on the ramp service provided by the unit; (19.k) and (19.l) constrain the sum of the generation and the ramp service within the generation capacity limits; (19.m) and (19.n) models the ramping limits. The system ramp-up and ramp-down requirements are set in (19.o) and (19.p). Equation (19.q) is the battery dynamic equation, and (19.r), (19.s) set the limitation on the battery energy. Battery operational limits are described in (19.t)–(19.w): (19.t) and (19.u) set the charging/discharging power of the battery storage as well as its ramp service within its charging/discharging limits; (19.v) and (19.w) regulate the battery ramp service within its capacity limits. Equation set (19.x) models the power flow equations and the transmission line flow limits. The extended distribution factor matrix \mathbf{H} represents the algebraic relationship between the branch flows and nodal power injections. It includes not only the regular transmission constraints but also N-1 contingencies and security constraints.

C. Considerations of the Unknowable Nature of the Extreme Events in the Proposed Formulations

In the proposed optimization model, the demand *reachability* ($Reach_{load}^{k,s}$) and generating unit *reachability* ($Reach_{gen}^{k,s}$) of each bus, especially their sequence, play an important role in

TABLE I
LIST OF THE GENERATING UNITS' START-UP PARAMETERS

Gen ID	Bus ID	Unit Type	T_{cp} (hr)	T_{cmin} (hr)	T_{cmax} (hr)	Rr (MW/min)	P_{start} (MW)
1, 2	1	U20	0	0:15	N/A	3	0
3, 4	1	U76	0	0:15	N/A	2	0
5, 6	2	U20	0:30	0	4:00	3	0.7
7, 8	2	U76	0:30	0	4:00	2	2.6
9-11	7	U100	2:00	0	3:30	7	3
12-14	13	U197	2:40	0:20	N/A	3	0.9
15	14	SC*	2:40	0:20	N/A	30	9
16-20	15	U12	2:00	0	N/A	1	0.7
21	15	U155	2:00	0	N/A	3	9
22	16	U155	1:40	0	N/A	3	3.1
23	18	U400	0:30	0	N/A	20	8
24	21	U400	0:30	0	N/A	20	8.8
25-30	22	U50	0	0	N/A	5	0
31-32	23	U155	1:40	0	2:50	3	3.1
33	23	U350	1:40	0	2:50	4	7

* Synchronous Condenser

maximizing the second and third objectives. The reason lies in the fact that the same amount of available capacity can achieve larger *capacity accessibility* if it is placed on a bus with higher *reachability*. However, the *reachability* of each bus can be quite different during the extreme events of different levels, resulting in different allocation strategies.

Considering the unknowable nature of extreme events, the idea is to: (1) calculate $Reach_{load}^{k,s}$ and $Reach_{gen}^{k,s}$ of each bus under extreme events of different levels, which can be simulated by altering $A_{event,s}$ within a certain range; (2) obtain the optimal sizing and siting scheme under each set of $Reach_{load}^{k,s}$ and $Reach_{gen}^{k,s}$; (3) average the attained optimal schemes to find the final allocation plan, as in (20).

$$\overline{B_{en/pow/pv}^k} = \left(\sum_{s \in S} B_{en/pow/pv}^k(A_{event,s}) \right) / N_s \quad (20)$$

where S is the set of all different levels of extreme events simulated; N_s is the number of extreme event levels in the set S ; $B_{en/pow/pv}^k(A_{event,s})$ is the allocation scheme (battery energy, battery power or PV generation, respectively) at bus k under $A_{event,s}$; and $\overline{B_{en/pow/pv}^k}$ is the final allocation scheme at bus k .

IV. NUMERICAL EXPERIMENTS AND ANALYSIS

A modified IEEE-RTS 24-bus test system is employed to illustrate the performance of the proposed framework. Detailed system configuration, including the bus connectivity and the unit parameters, is in [35]. Load profile and solar data are collected from the ERCOT system [36] and the California Irrigation Management Information System [37], respectively.

A. Prioritizing the NB-S Generating Units

During the B-S process, the hydro units located on bus 22 are treated as the B-S units, while the others are regarded as NB-S units. Table. I lists the start-up parameters of the units. Fig. 3 demonstrates the starting time of the NB-S units during the B-S process with participation of all generating units. Also, the priority of each NB-S unit characterized by (11)

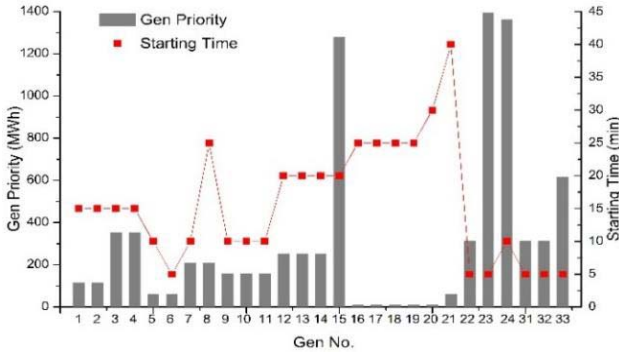


Fig. 3. The priority and starting time of the generating units.

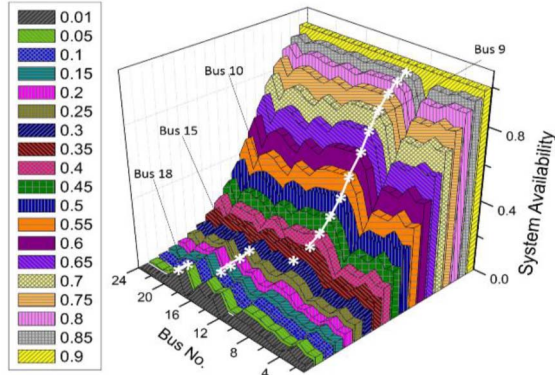


Fig. 4. Demand reachability ($Reach_{load}^k$) of each bus under events of different intensity levels.

is illustrated. One can observe, from Fig. 3, that the importance of the NB-S units during the B-S process does not solely depend on their power capacity, but also affected by other factors such as: (a) starting time: early start-up results in higher priority (No. 21 vs. 22); (b) the value of T_{cip} : the longer T_{cip} causes lower priority (No.1, 2 vs. No. 5, 6, and No. 3, 4 vs. No. 7, 8); (c) the value of P_{start} : larger P_{start} leads to lower priority; and (d) ramp rates: higher ramp rate results in higher priority. The reason behind (c) and (d) is that the NB-S units with higher ramp rate and lower P_{start} tend to start earlier than the others, with the constraints on T_{cmin} and T_{cmax} satisfied.

B. Demand/Generating Unit Reachability Under Extreme Events

Having recognized the priority of each NB-S unit, $Reach_{load}^k$ (5) and $Reach_{gen}^k$ (10) can be calculated for each bus under events of different levels, as illustrated in Fig. 4 and Fig. 5, respectively. To illustrate the events of different levels (from light to extremely severe), $A_{event,s}$ is varied from 0.01 to 0.9, with the interval of 0.05. To simplify the problem, the adjusting coefficient ζ is assumed to be 1. One can see that the reachability decreases as $A_{event,s}$ decreases (more severe). The reachability of all buses is 1 (no island) when $A_{event,s}$ exceeds 0.9 and higher (that is why the upper limit for $A_{event,s}$ is selected to be 0.9). The white stars in the aforementioned two figures denote the bus with the highest reachability in each case. Those stars connected with lines reflect the fact that the highest reachability is achieved on the same bus. The results

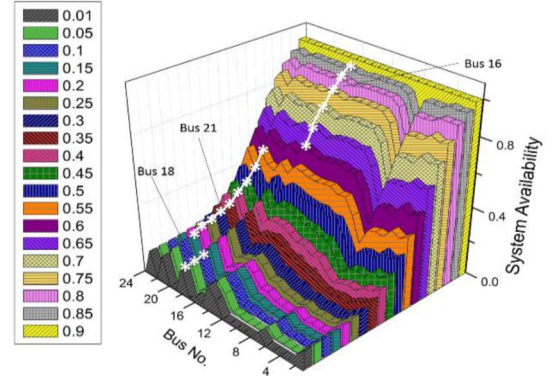


Fig. 5. Generating unit reachability ($Reach_{gen}^k$) of each bus under events of different intensity levels.

TABLE II
LIST OF GENERATION COST AND RAMP COST

Unit Type	C_G (\$/MWh)	C_{FRU}, C_{FRD} (\$/MWh)
U12	85	15
U20	90	15
U50	7	20
U76	31	15
U100	75	15
U155	27	20
U197	70	17
U350	25	15
U400	15	16

demonstrate that: (1) the bus with the highest reachability varies among the events of different levels. Therefore, various events of different levels need to be considered when determining the optimal sizing and siting scheme; (2) the bus with the highest demand reachability may not be the one with the highest generating unit reachability. It confirms the need for a multi-objective optimization approach; (3) buses with the highest reachability levels remain the same when $A_{event,s}$ changes within a certain range, and therefore, the selection of the 0.05 interval for $A_{event,s}$ would not miss any important buses. The lower bound of $A_{event,s}$ is determined to be 0.01, as the important buses remain the same when $A_{event,s}$ is lower.

C. Optimal Sizing and Siting Scheme

The proposed optimization is conducted considering the events with $A_{event,s}$ ranging from 0.01 to 0.85. The costs related to the generators are listed in Table. II, in which the generation cost is calculated from [35]. r and L_p in (15.b) are assumed to be 0.25 and 10, respectively. C_{BG} is selected to be 50; C_{BFRU} and C_{BFRD} are considered to be 5.44 [31]. $C_{energy}^{B_{in}}$, $C_{power}^{B_{in}}$ and $C_{pv_{in}}$ are calculated from [38]. The proposed formulation is a mixed-integer linear optimization model and is solved by CPLEX V12.5 in MATLAB (R2011a) environment on an Intel i5 1.6-GHz processor (8 GB of memory), with the computation time of about 23 mins per case. Fig. 6 illustrates the Pareto Front resulted from the proposed scheme. The value of lost load, assumed to be \$3500/MWh [39], is utilized to convert the second and third objectives into monetary values. Besides, these two objectives are transformed into minimization problems through their additive inverse, and therefore, are in negative numbers.

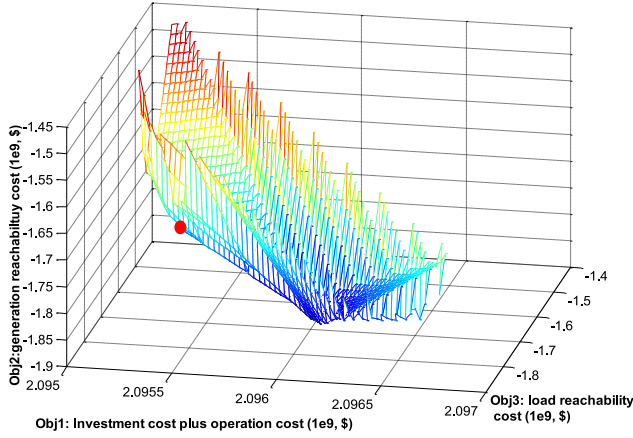


Fig. 6. Pareto front of the optimal sizing and siting scheme.

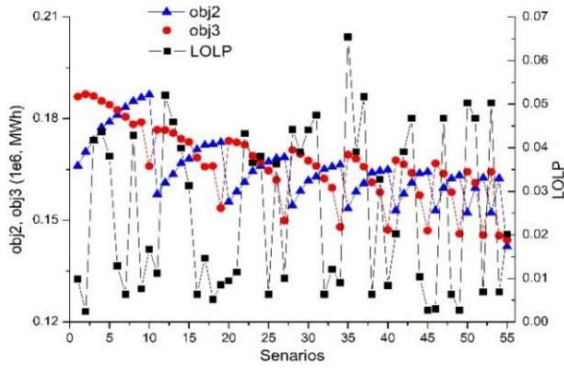


Fig. 7. Illustration of the LOLP and capacity availability.

This figure illustrates the trade-off between the economic cost and resilience, and provides a reference for the planning decision.

Meanwhile, we conduct the N-1 and N-2 reliability analysis (failure of any one or two elements in the system) on some of the optimal solutions in Fig. 6. The index of Loss of Load Probability (LOLP) is utilized to evaluate the system reliability performance by reflecting the probability that the load interruption occurs in the system. It is calculated in (21), where Π is the set of single-order and second-order contingencies; y_z is a binary variable indicating whether the system experiences any load interruption (0: no load interruption; 1: load interruption); the contingency probability P_{rob}^z is calculated using the equipment failure probabilities.

$$LOLP = \sum_{z \in \Pi} y_z \cdot P_{rob}^z \quad (21)$$

Accordingly, Fig. 7 illustrates the result of LOLP indices as well as the system-wide *capacity accessibility* for both electricity demand and NB-S generating units (i.e., values of obj. 2 & obj. 3). The system LOLP in the base case scenario is 0.82. From Fig. 7, one can observe that the installation of PV and the battery storage does improve the system reliability, as the updated LOLP is lower. However, no distinct correlation between the LOLP and the *capacity accessibility* can be observed. This highlights that (1) the proposed *capacity accessibility* metric is different from the concept of reliability;

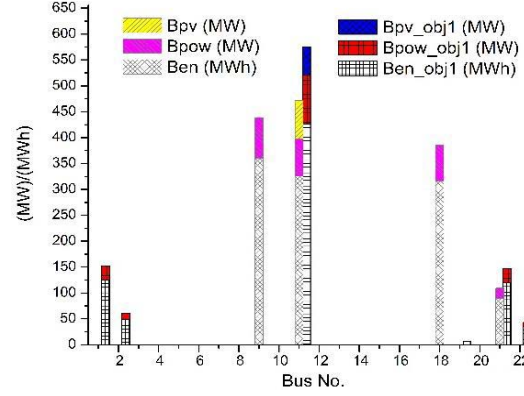


Fig. 8. Detailed illustration of the optimal sizing and siting solutions.

 TABLE III
 DETAILED INFORMATION ON THE STUDIED CONTINGENCIES

ID	Gen. in fault	Lines in fault	Gen. start-up
1	U23, U24	None	U13
2	U23, U24	None	None
3	U23, U24, U33	2, 3, 6	None
4	U23, U24, U33	2,3,6,10	None
5	U3, U4, U23, U24, U33	2, 3, 6, 10, 15, 16	None
6	U3, U4, U23, U24, U33	2,3,6,10,15,16,18,19,25,26,31	None

and (2) the improvement in system reliability cannot guarantee the improvement on the *capacity accessibility* and system-wide resilience in face of extreme events.

The detailed placement solutions for the result denoted in the red dot in Fig. 6 are illustrated in Fig. 8, together with the case with a conventional placement scheme that just considers the cost in obj.1 (15.a). One can observe that the proposed placement solution tends more to place the resources on the buses with the highest $Reach_{load}^k$ or $Reach_{gen}^k$, compared with the other case (obj.1). The resource on bus 11 is an exception, which also considers the operation requirements.

In order to evaluate the impact of the placement of the battery storage and the PV generation on system resilience, especially on the load pick-up process, several contingencies are simulated and the reaction of the system is studied. The contingencies are assumed to occur on a certain day at hour 11 and last for 2 hours. The detailed information of the studied contingencies is illustrated in Table. III, in the order from light to severe. The ENS associated with the proposed placement solution and the one with neither battery nor PV generation available are illustrated in Fig. 9 under different contingency scenarios. In addition, Fig. 10 shows: (1) the differences in ENS of all other placement cases under each contingency scenario, compared with that of the proposed case; and (2) the Mean Absolute Error (MAE) of the differences in ENS under each contingency scenario. Other than the placement solution obtained through obj.1 alone (see Fig. 8), additional sizing and siting cases are compared. Case i denotes that the resources obtained by the proposed method are all placed on the bus i .

From Fig. 9 and Fig. 10, one can see that: (1) installation of the PV and the battery storage does help reducing the ENS during contingencies; and (2) the proposed placement solution gradually shows its obvious advantage over the other placement schemes where the contingency tends to be

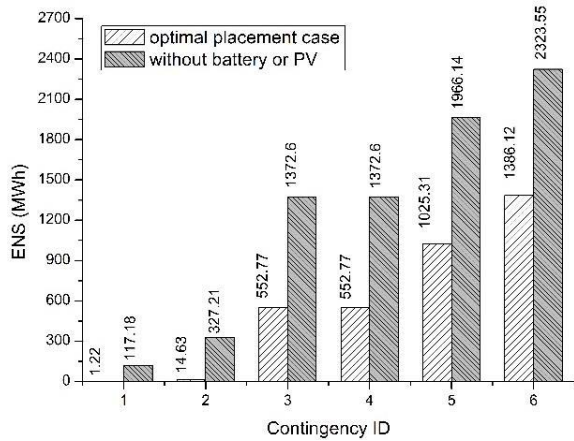


Fig. 9. ENS of the system under difference contingencies.

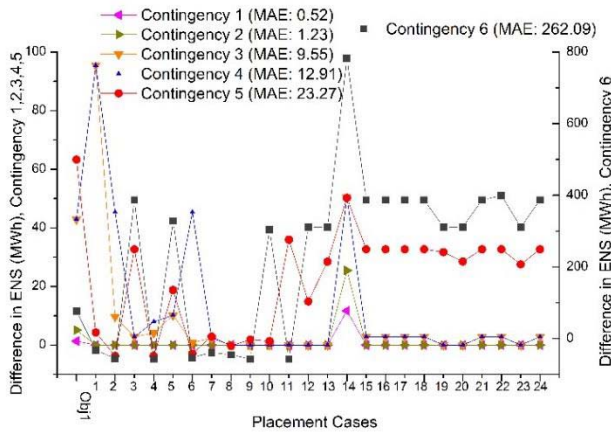


Fig. 10. Differences in ENS corresponding to different placement schemes.

TABLE IV
DETAILED RESULTS OF THE ENS UNDER
VARIOUS ALLOCATION SCHEMES

ID	Obj1		No PV generation	
	ENS(MWh)	Difference(MWh)	ENS(MWh)	Difference(MWh)
1	2.54	1.32	4.92	3.71
2	19.77	5.14	33.68	19.04
3	595.71	42.94	683.33	130.55
4	595.71	42.94	683.33	130.55
5	1088.62	63.31	1196.76	171.45
6	1463.37	77.26	1578.28	192.16

* Note: the ENS under the proposed case is set as the reference to generate the "Difference" in Table IV.

more extreme (the variations and the MAEs in Fig. 10 increase when the contingency is more severe). In order to more clearly demonstrate the difference in the ENS between the two cases shown in Fig. 8, and to highlight the role of the PV generation, additional results are tabulated in Table. IV*. In the case of "No PV generation", the solar generation is removed from the proposed placement solution. The results demonstrate that the PV generation, although not installed in a large capacity, is also playing an important role in helping recovering the load, especially when the contingency tends to be more extreme.

Last but not the least, the impact of different placement schemes on the B-S process, which is another critical aspect of system resilience, is evaluated in terms of the pick-up energy in Fig. 11. One can observe that: (1) the integration of battery

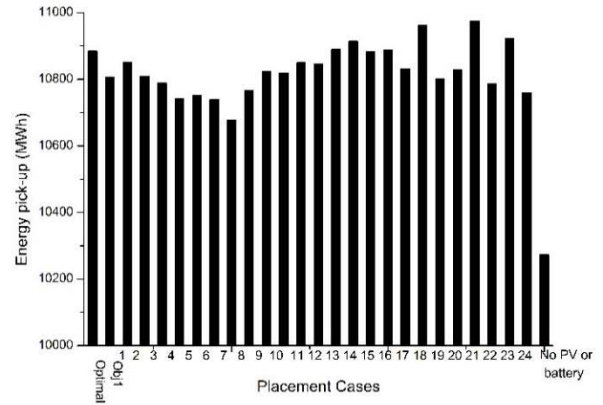


Fig. 11. Energy pick-up during the black-start process.

storage and PV generation helps restore more energy during the B-S process; (2) more energy can be picked up under the proposed placement solution compared with the one that just considers the investment and operational cost (obj.1); and (3) the pick-up energy under the proposed scheme, although not the highest, is higher than most of the other allocation cases.

V. CONCLUSION

This paper investigates an optimal placement scheme for battery storage and PV generation to be more accessible for both the load and NB-S units in face of extreme events, aiming at enhancing the system resilience. We introduced the concepts of *reachability* and index of *capacity accessibility* to help identifying some critical buses and framing the objectives in a multi-objective sizing and siting optimization paradigm. It is found in the numerical experiments that some buses are quite more critical than others, since resources placed on those buses can be more reachable by the loads or NB-S units during extreme events of different intensity levels. Following the proposed optimal sizing and siting scheme, the system has better performance in terms of load pick-up and the B-S process expedition during extreme events, compared with other placement schemes. The difference becomes more obvious when the contingency tends to be more extreme.

The main contributions of the paper are:

- 1) A new concept of *reachability* is proposed enabling the simulation of the impact of extreme events of different intensity levels on power systems;
- 2) Metrics of *capacity accessibility* for both demand and NB-S generating unit are proposed which allows the evaluation of the *capacity adequacy* during extreme events, considering the priority of the NB-S generating units in terms of their criticality in the B-S process;
- 3) A new multi-objective optimization model is formulated to find the optimal sizing and siting scheme for the battery storage and PV generation, aiming at improving the system resilience through increasing the system-wide *capacity accessibility*, taking into account the unknowable nature of the extreme events and costs;
- 4) Numerical experiments are conducted to verify the effectiveness of the proposed approach in improving the system resilience.

Future research may include a detailed physical modeling of PV and storage units to be incorporated in the proposed optimization framework. Other aspects of system resilience, e.g., transmission line energization, load pickup, and system stability, should be also further studied and efficiently embedded in the suggested optimization scheme.

REFERENCES

- [1] S. Frueh. (Jul. 25, 2014). *Improving Power System Resilience in the 21st Century Resilient America Roundtable*. Accessed: Jan. 21, 2017. [Online]. Available: http://sites.nationalacademies.org/cs/groups/pgasite/documents/webpage/pga_153420.pdf
- [2] NERC. (Oct. 15, 2015). *2015 Risk Element: Extreme Physical Events Industrial Webinar*. Accessed: Jan. 21, 2017. [Online]. Available: <http://www.nerc.com/pa/comp/Documents/2015%20Extreme%20Physical%20Events%20v1.08.pdf>
- [3] M. Panteli and P. Mancarella, "The grid: Stronger, bigger, smarter?: Presenting a conceptual framework of power system resilience," *IEEE Power Energy Mag.*, vol. 13, no. 3, pp. 58–66, May/June. 2015.
- [4] M. Panteli and P. Mancarella, "Modeling and evaluating the resilience of critical electrical power infrastructure to extreme weather events," *IEEE Syst. J.*, to be published, doi: 10.1109/JSYST.2015.2389272. [Online]. Available: <http://ieeexplore.ieee.org/stamp/stamp.jsp?arnumber=7036086>
- [5] M. Panteli and P. Mancarella, "Operational resilience assessment of power systems under extreme weather and loading conditions," in *Proc. IEEE PES Gen. Meeting*, Denver, CO, USA, 2015, pp. 1–5.
- [6] D. Barus, "Implementation of free governor action in power plant to increase system resilience of Jawa Bali power system network," in *Proc. 46th Int. Univ. Power Eng. Conf. (UPEC)*, Soest, Germany, 2011, pp. 1–5.
- [7] Y. Liu, Q. H. Wu, and X. X. Zhou, "Co-ordinated multiloop switching control of DFIG for resilience enhancement of wind power penetrated power systems," *IEEE Trans. Sustain. Energy*, vol. 7, no. 3, pp. 1089–1099, Jul. 2016.
- [8] K. Eshghi, B. K. Johnson, and C. G. Rieger, "Power system protection and resilient metrics," in *Proc. IEEE Resilience Week*, Philadelphia, PA, USA, 2015, pp. 1–8.
- [9] T. C. Ly, J. N. Moura, and G. Velumylym, "Assessing the bulk power system's resource resilience to future extreme winter weather events," in *Proc. IEEE Power Energy Soc. Gen. Meeting*, Denver, CO, USA, 2015, pp. 1–4.
- [10] Y. Sun, Z. Li, M. Shahidehpour, and B. Ai, "Battery-based energy storage transportation for enhancing power system economics and security," *IEEE Trans. Smart Grid*, vol. 6, no. 5, pp. 2395–2402, Sep. 2015.
- [11] N. Kadel, W. Sun, and Q. Zhou, "On battery storage system for load pickup in power system restoration," in *Proc. IEEE Power Energy Soc. Gen. Meeting*, National Harbor, MD, USA, 2014, pp. 1–5.
- [12] W. Liu, L. Sun, Z. Lin, F. Wen, and Y. Xue, "Multi-objective restoration optimisation of power systems with battery energy storage systems," *IET Gener. Transm. Distrib.*, vol. 10, no. 7, pp. 1749–1757, May 2016.
- [13] Y. Zheng *et al.*, "Optimal allocation of energy storage system for risk mitigation of DISCOs with high renewable penetrations," *IEEE Trans. Power Syst.*, vol. 29, no. 1, pp. 212–220, Jan. 2014.
- [14] M. A. Darfoun and M. E. El-Hawary, "Multi-objective optimization approach for optimal distributed generation sizing and placement," *Elect. Power Compon. Syst.*, vol. 43, no. 7, pp. 828–836, Apr. 2015.
- [15] A. S. A. Awad, T. H. M. El-Fouly, and M. M. A. Salama, "Optimal ESS allocation and load shedding for improving distribution system reliability," *IEEE Trans. Smart Grid*, vol. 5, no. 5, pp. 2339–2349, Sep. 2014.
- [16] H. Gao, Y. Chen, S. Mei, S. Huang, and Y. Xu, "Resilience-oriented pre-hurricane resource allocation in distribution systems considering electric buses," *Proc. IEEE*, vol. 105, no. 7, pp. 1214–1233, Jul. 2017. [Online]. Available: <http://ieeexplore.ieee.org/stamp/stamp.jsp?arnumber=7879853>
- [17] M. Ghofrani, A. Arabali, M. Etezadi-Amoli, and M. S. Fadali, "A framework for optimal placement of energy storage units within a power system with high wind penetration," *IEEE Trans. Sustain. Energy*, vol. 4, no. 2, pp. 434–442, Apr. 2013.
- [18] M. Ghofrani, A. Arabali, M. Etezadi-Amoli, and M. S. Fadali, "Energy storage application for performance enhancement of wind integration," *IEEE Trans. Power Syst.*, vol. 28, no. 4, pp. 4803–4811, Nov. 2013.
- [19] L. Zheng, W. Hu, Q. Lu, and Y. Min, "Optimal energy storage system allocation and operation for improving wind power penetration," *IET Gener. Transm. Distrib.*, vol. 9, no. 16, pp. 2672–2678, Dec. 2015.
- [20] C. Thrampoulidis, S. Bose, and B. Hassibi, "Optimal placement of distributed energy storage in power networks," *IEEE Trans. Autom. Control*, vol. 61, no. 2, pp. 416–429, Feb. 2016.
- [21] H. Pandžić, Y. Wang, T. Qiu, Y. Dvorkin, and D. S. Kirschen, "Near-optimal method for siting and sizing of distributed storage in a transmission network," *IEEE Trans. Power Syst.*, vol. 30, no. 5, pp. 2288–2300, Sep. 2015.
- [22] S. Wogrin and D. F. Gayme, "Optimizing storage siting, sizing, and technology portfolios in transmission-constrained networks," *IEEE Trans. Power Syst.*, vol. 30, no. 6, pp. 3304–3313, Nov. 2015.
- [23] V. Krishnan and T. Das, "Optimal allocation of energy storage in a co-optimized electricity market: Benefits assessment and deriving indicators for economic storage ventures," *Energy*, vol. 81, pp. 175–188, Mar. 2015.
- [24] R. Fernández-Blanco, Y. Dvorkin, B. Xu, Y. Wang, and D. S. Kirschen. (Jun. 2016). *Energy Storage Siting and Sizing in the WECC Area and the CAISO System*. [Online]. Available: https://www2.ee.washington.edu/research/real/Library/Reports/storage_siting_and_sizing.pdf
- [25] M. Motalleb, E. Reihani, and R. Ghorbani, "Optimal placement and sizing of the storage supporting transmission and distribution networks," *Renew. Energy*, vol. 94, pp. 651–659, Aug. 2016.
- [26] H. Yu, J. Pan, and A. Xiang, "A multi-function grid-connected PV system with reactive power compensation for the grid," *Solar Energy*, vol. 79, no. 1, pp. 101–106, 2005.
- [27] S. Adhikari and F. Li, "Coordinated V-f and P-Q control of solar photovoltaic generators with MPPT and battery storage in microgrids," *IEEE Trans. Smart Grid*, vol. 5, no. 3, pp. 1270–1281, May 2014.
- [28] L. Jiang and Q. Yang, "Intelligent power supply restoration in power distribution networks with distributed generation," in *Proc. IEEE China Int. Conf. Electricity Distrib. (CICED)*, Xi'an, China, Aug. 2016, pp. 1–6.
- [29] C. Velásquez, D. Watts, H. Rudnick, and C. Bustos, "A framework for transmission expansion planning: A complex problem clouded by uncertainty," *IEEE Power Energy Mag.*, vol. 14, no. 4, pp. 20–29, Jul./Aug. 2016.
- [30] W. Sun, C.-C. Liu, and L. Zhang, "Optimal generator start-up strategy for bulk power system restoration," *IEEE Trans. Power Syst.*, vol. 26, no. 3, pp. 1357–1366, Aug. 2011.
- [31] B. Zhang and M. Kezunovic, "Impact on power system flexibility by electric vehicle participation in ramp market," *IEEE Trans. Smart Grid*, vol. 7, no. 3, pp. 1285–1294, May 2016.
- [32] M. Moeini-Aghaie, A. Abbaspour, and M. Fotuhi-Firuzabad, "Incorporating large-scale distant wind farms in probabilistic transmission expansion planning—Part I: Theory and algorithm," *IEEE Trans. Power Syst.*, vol. 27, no. 3, pp. 1585–1593, Aug. 2012.
- [33] A. Arabali, M. Ghofrani, M. Etezadi-Amoli, M. S. Fadali, and M. Moeini-Aghaie, "A multi-objective transmission expansion planning framework in deregulated power systems with wind generation," *IEEE Trans. Power Syst.*, vol. 29, no. 6, pp. 3003–3011, Nov. 2014.
- [34] Y. M. Atwa, E. F. El-Saadany, M. M. A. Salama, and R. Seethapathy, "Optimal renewable resources mix for distribution system energy loss minimization," *IEEE Trans. Power Syst.*, vol. 25, no. 1, pp. 360–370, Feb. 2010.
- [35] C. Grigg *et al.*, "The IEEE reliability test system-1996. A report prepared by the reliability test system task force of the application of probability methods subcommittee," *IEEE Trans. Power Syst.*, vol. 14, no. 3, pp. 1010–1020, Aug. 1999.
- [36] ERCOT Balancing Energy Services Daily Reports Archives. (2008). *Balancing Energy Services Daily Reports*. [Online]. Available: <http://www.ercot.com/mktinfo/services/bal/2008/index>
- [37] California Irrigation Management Information System (CIMIS). [Online]. Available: <http://www.cimis.water.ca.gov/>
- [38] L. Xu, X. Ruan, C. Mao, B. Zhang, and Y. Luo, "An improved optimal sizing method for wind-solar-battery hybrid power system," *IEEE Trans. Sustain. Energy*, vol. 4, no. 3, pp. 774–785, Jul. 2013.
- [39] A. A. Thatte, X. A. Sun, and X. Le, "Robust optimization based economic dispatch for managing system ramp requirement," in *Proc. Hawaii Int. Conf. Syst. Sci.*, Waikoloa Village, HI, USA, 2014, pp. 2344–2352.